

GROUND-STATE CORRELATIONS AND FINAL STATE
INTERACTIONS IN THE PROCESS ${}^3\text{H} e(e;e^0 pp)n$

C. Cio degli Atti and L.P. Kaptari

Department of Physics, University of Perugia, and INFN,
Sezione di Perugia, via A. Pascoli, Perugia, I-06100, Italy

(Dated: October 25, 2019)

The two-proton emission process from ${}^3\text{H} e$ is analyzed using realistic three-nucleon wave functions and taking the final state interaction into account. Various kinematical conditions are considered in order to check whether the effects of the final state interaction can be minimized by a proper choice of the kinematics.

arXiv:nucl-th/0203041v1 17 Mar 2002

I. INTRODUCTION

The investigation of ground-state Correlations (GSC) in nuclei, in particular those which originate from the most peculiar features of the Nucleon-Nucleon (NN) interaction, i.e. its strong short range repulsion and complex state dependence (spin, isospin, tensor, etc), is one of the most challenging aspects of experimental and theoretical nuclear physics and, more generally, of hadronic physics. The results of sophisticated few- and many-body calculations in terms of realistic models of the NN interaction ([1, 2, 3]) show that the complex structure of the latter generates a rich correlation structure of the nuclear ground-state wave function. The experimental investigation of the nuclear wave function or, better, of various density matrices, $(1); (1;1^{\dagger}); (1;2);$ etc, is therefore necessary in order to ascertain whether the prediction of the Standard Model of nuclei (structureless non-relativistic nucleons interacting via the known NN forces) is indeed justified in practice, or other phenomena, e.g., relativistic effects, many-body forces, medium modification of nucleon properties, and explicit sub-nucleonic degrees of freedom (quark and gluons), have to be advocated in order to describe ground-state properties of nuclei at normal density and temperature.

Unfortunately, whereas the one-body density matrix (charge density) is experimentally well known since many years from elastic electron scattering (see e.g. [4]), the present knowledge of those quantities which are more sensitive to GSC, e.g. the non-diagonal one-body and two-body density matrices, which could in principle be investigated by semi-inclusive and exclusive processes like e.g. the $A(e;e^{\dagger}N)X$ and $A(e;e^{\dagger}NN)X$ reactions, where one or more nucleons (N) are detected in coincidence with the scattered electron, is still too scarce. The reason is that the effects of the final state interaction (FSI), Meson Exchange Currents (MEC) and Isobar Configuration (IC) creation, may mask the effects generated by GSC. In our view, the present situation is such that the longstanding question whether FSI and other concurrent processes hinder the investigation of GSC, has not yet been clearly answered. Moreover, due to the difficulty to treat consistently GSC, FSI, MEC, etc within the full complexity of the nuclear many-body approach, the answer to the above question was in the past merely dictated by philosophical taste rather than by the results of solid calculations and unambiguous experimental data. A clear cut answer to the above question, would require, from one side, realistic many-body calculations of bound and continuum nuclear states, and, from the other side, a wise choice of the type of process to be investigated, so as to possibly

minimize all those effects which compete with GSC. These requirements clearly points to the necessity of performing experiments and theoretical calculations in the few-body systems domain, where accurate ground-state wave functions are available and FSI effects can also be calculated in a satisfactory way (see e.g. [5, 6, 7] and References therein quoted). As for the choice of the process, it is well known (see e.g. [8], [9]) that in the two-proton emission process $A(e;e^0pp)X$, MEC play a minor role (with respect to the proton-neutron emission $A(e;e^0pn)X$), since the virtual photon does not couple to the exchanged neutral meson, and that because of angular momentum and parity conservation selection rules, also IC production is suppressed. Extensive theoretical studies on the $A(e;e^0pp)X$ process on complex nuclei have been performed (see e.g. [10, 11, 12], and References therein quoted) and experimental data on complex nuclei (see e.g. [13], [14]) have also appeared, but we will discuss complex nuclei in a subsequent paper, for we intend here to concentrate on the case of few-body systems, following our believe that its understanding is a prerequisite for understanding the process in complex nuclei. Experiments on the ${}^3\text{H}e(e;e^0pp)n$ reaction have already been performed at NIKHEF ([15]) and are being investigated at the Thomas Jefferson National Facility (TJNAF) using the CEBAF Large Acceptance Spectrometer (CLAS), which allows one to completely determine the full kinematics of the process ([16], [17]). The aim of the present paper is to thoroughly discuss the problem whether by a proper choice of the kinematics, the effects of FSI in the process ${}^3\text{H}e(e;e^0pp)n$ can be minimized. Preliminary results of our calculations have already been presented in Ref. [18]. Through this paper we shall be using the three body wave functions obtained by the Pisa Group [7, 19].

Our paper is organized as follows: in Section II the most general concept concerning the Kinematics of the process and the Cross Section will be recalled; our approach to the treatment of FSI is illustrated in Section III together with the results of calculations; the Summary and Conclusions are given in Section IV. Some useful formulae are given in the Appendix.

II. KINEMATICS AND CROSS SECTION

We will consider the absorption of a virtual photon by a nucleon bound in ${}^3\text{H}e$, followed by two-nucleon emission, i.e. the process ${}^3\text{H}e(e;e^0N_1N_2)N_3$, where N_1 and N_2 denote the nucleons which are detected. In the rest of this paper the photon four momentum transfer

will be denoted by

$$Q^2 = \hat{q}^2 = (\mathbf{k} - \mathbf{k}_0)^2 = q^2 = 4 m_e m_{e^0} \sin^2 \frac{\theta}{2} \quad (1)$$

where $\mathbf{k} = (\mathbf{k}; k)$ is the four momentum of the electron, $q = |\mathbf{k} - \mathbf{k}_0|$, $m_e = m_{e^0}$ and $m_e = k_e k_{e^0}$.

The momenta of the bound nucleons, before absorption, will be denoted by k_i , and after absorption, by p_i . Momentum conservation requires that

$$\sum_{i=1}^3 k_i = 0 \quad \sum_{i=1}^3 p_i = q \quad (2)$$

and energy conservation that

$$E + M_3 = \sum_{i=1}^3 (M_N^2 + p_i^2)^{1/2} \quad (3)$$

where M_N and M_3 are the masses of the nucleon and the three-nucleon system, respectively.

In one-photon exchange approximation, depicted in Fig. 1, the cross section of the process, reads as follows

$$\frac{d^4\sigma}{d\omega d\Omega d\mathbf{p}_1 d\mathbf{p}_2 d\mathbf{p}_3} = \frac{1}{M_{\text{ott}}} \sum_{i=1}^3 v_i W_i(q, \mathbf{p}_i) \left(E + M_3 + \sum_{i=1}^3 (M_N^2 + p_i^2)^{1/2} \right) \quad (4)$$

where v_i are well known kinematical factors, and W_i the response functions, which have the following general form

$$W_i = h_f^{(i)}(\mathbf{p}_1; \mathbf{p}_2; \mathbf{p}_3) \hat{\mathcal{O}}_i(\mathbf{q}) j_i(\mathbf{k}_1; \mathbf{k}_2; \mathbf{k}_3) i_i^2 \quad (5)$$

In Eq.5 $h_f^{(i)}(\mathbf{p}_1; \mathbf{p}_2; \mathbf{p}_3)$ and $i_i(\mathbf{k}_1; \mathbf{k}_2; \mathbf{k}_3)$ are the continuum and ground-state wave functions of the three-body system, respectively, and $\hat{\mathcal{O}}_i(\mathbf{q})$ is a quantity depending on proper combinations of the components of the nucleon current operator \hat{j} (see e.g. [4]). Two nucleon emission originated by NN correlations can occur because of two different processes:

1. in the initial state "1" and "2" are correlated and "3" is far apart; ω is absorbed either by "1" or "2" and all of the three nucleons are emitted in the continuum; if nucleon "3" was at rest in the initial state, one has $k_1 = -k_2$ and, if FSI is disregarded, $p_{1(2)} = k_{1(2)} + q$, $p_{2(1)} = k_{2(1)}$ in the final state;

2. in the initial state nucleons "1" and "2" are correlated and "3" is far apart; is absorbed by N_3 and all of the three nucleons are emitted in the continuum. If N_3 was at rest before interaction, and FSI is disregarded, N_1 and N_2 are emitted back-to-back with momenta $k_1 = -k_2$ and $p_3 = q$.

The above picture is distorted by FSI. The aim of this paper is precisely to investigate the relevance of FSI effects in both processes.

III. THE FINAL STATE INTERACTION IN THE TWO-NUCLEON EMISSION PROCESS

We will now assume that N_1 and N_2 , the two detected nucleons, are the two protons and N_3 the neutron (n). The two-nucleon emission process will thus be ${}^3\text{H}(e; e^0 p_1 p_2)n$ which, as explained, can originate from the two mechanisms described above.

A. Process 1: absorption of q by the correlated pp pair.

In this process q is absorbed by proton "1" ("2") correlated with proton "2" ("1"), and the neutron is the "spectator".

The various diagrams, in order of increasing complexity, which contribute to the process, are depicted in Fig. 2.

Let us introduce the following quantities:

1. the relative momentum of the detected proton pair

$$p_{\text{rel}} = \frac{p_1 - p_2}{2} \quad t \quad (6)$$

2. the Center-of-Mass momentum of the pair

$$P = p_1 + p_2 \quad (7)$$

In what follows, for ease of presentation and also in order to make the comparison with previous calculations more transparent, we will consider the effects of the FSI on the longitudinal response only. Let us first consider diagrams a) and b), i.e. the Plane Wave

Approximation plus the pp rescattering in the final state. By changing the momentum variables from p_1 and p_2 to P and p_{rel} , and integrating the cross section (Eq. (4)) over P and the kinetic energy of the neutron, we obtain

$$\frac{d^8}{d_e^0 d_e^0 d_{p_n} d_{p_{rel}} d_{P_{rel}}} = K(Q^2; p_n; p_{rel}) R(Q^2; p_n; p_{rel}) \quad (8)$$

with

$$R_L(Q^2; p_n; p_{rel}) = G_E^p(Q^2)^2 M^{(pp)}(p_n; p_{rel}; q) \quad (9)$$

where $G_E(Q^2)$ is the proton electric form factor, K incorporates all kinematical variables, and $M^{(pp)}(p_n; p_{rel}; q)$ is the transition nuclear form factor which includes the pp rescattering, viz

$$M^{(pp)}(p_n; p_{rel}; q) = \frac{1}{2} \sum_{M} \sum_{S_{pp}; pp} \sum_{\chi_n} \int T^{(pp)}(M; \chi_n; S_{pp}; pp; p_n; p_{rel}; q) \quad (10)$$

The scattering matrix $T^{(pp)}(M; \chi_n; S_{pp}; pp; p_n; p_{rel}; q)$ has the following form

$$\int_{\mathbb{Z}} T^{(pp)}(M; \chi_n; S_{pp}; pp; p_n; p_{rel}; q) = \int d^3 r d^3 \left(\frac{1}{2} M(r; \chi_n) \exp(i p_n \cdot r) \right) S_{pp; pp}^t(r) \exp(i q r = 2); \quad (11)$$

where $\frac{1}{2} M(r; \chi_n)$ is the three-nucleon wave function, $S_{pp; pp}^t(r)$ the continuum two-proton wave function, and $\frac{1}{2} \chi_n$ the neutron spinor.

When pp rescattering is disregarded, i.e. only diagram a) is considered, one has

$$p_1 = k_1 + q \quad p_2 = k_2 \quad p_n = k_n \quad (12)$$

$$p_{rel} = k_{rel} + \frac{q}{2} \quad P = K + q \quad (13)$$

where

$$k_{rel} = \frac{k_1 - k_2}{2} \quad K = k_1 + k_2 = k_n \quad (14)$$

are the relative and CM momenta of the pp pair before interaction. The two-proton continuum wave function is simply $S_{pp; pp}^t(r) = S_{pp; pp} \exp(i p_{rel} \cdot r)$ and the scattering amplitude

becomes

$$\frac{T}{Z}^{(pp)}(M; n; S_{pp}; p_n; p_{rel}; q) \neq T^{(PW A)}(M; n; S_{pp}; p_n; k_n; k_{rel}) = \int d^3r d^3r' \frac{1}{2} M(r; r') \frac{1}{2} n \exp(-ik_n r) S_{pp}; p_n \exp(-ik_{rel} r); \quad (15)$$

which is nothing but the three-body wave function in momentum space.

In the above and the following equations, r and r' are the Jacobi coordinates

$$r = r_1 \quad r' = r_3 \quad = r_3 \quad \frac{1}{2} (r_1 + r_2) \quad (16)$$

which are related to the nucleon co-ordinates as follows

$$r_1 = \frac{1}{3} + \frac{1}{2} r + R \quad (17)$$

$$r_2 = \frac{1}{3} - \frac{1}{2} r + R \quad (18)$$

$$r_3 = + \frac{2}{3} + R \quad (19)$$

where $R = \frac{1}{3} \sum_{i=1}^3 r_i$ is the CM coordinate.

The scattering amplitude which include the pp rescattering has been calculated using the continuum wave function for two interacting protons

$$t_{S_{pp}; p_n}^{(pp)}(r) = 4 \sum_{l m} \sum_{l' m'} S_{pp} \sum_{j_f M_j} \sum_{j_i M_i} Y_{l m}(\hat{\phi}_{rel}) R_{l S^0}^{j_f}(\mathbf{r}) Y_{l' m'}^{j_i M_j}(\hat{\mathbf{r}}); \quad (20)$$

where $Y_{l m}(\hat{\phi}_{rel}) Y_{l' m'}^{j_i M_j}(\hat{\mathbf{r}})$ denotes the spherical (spin-angular) harmonics, and $R_{l S^0}^{j_f}(\mathbf{r})$ is the scattering radial wave function, solution of the Schrodinger equation in the continuum, with asymptotic behaviour

$$R_{l S^0}^{j_f}(\mathbf{r}) \sim \frac{1}{r^{l+1}} \exp(i k r) \frac{\sin [k r - (l+1/2)\pi]}{k r} \quad (21)$$

where $t = j_j - j_{rel}$. In the presence of a tensor interaction the asymptotic of $R_{l S^0}^{j_f}(\mathbf{r})$ is more complicated but, by a unitary transformation, other radial wave functions may be introduced with asymptotic similar to eq. (21) (see e.g. Ref. [20]).

Inserting (20) into (11), and using the completeness of the scattering wave functions, the amplitude $T^{(pp)}$ in Eq. (10) can be expressed in the following way

$$\begin{aligned}
 T^{(pp)}(M; n; S_{pp}; p_n; p_{rel}; q) &= \frac{2}{\pi} \int_0^{\infty} dt \int d^3r \exp(i p_n \cdot r) \\
 &\times \int_{f, g} h_{L M}^{j_1 M} \frac{1}{2} i h_{j_1 2}^{j_2 M} \frac{1}{2} \int_{f, g} h_{L M}^{j_1 M} i \\
 &h_{j_1 2}^{j_2 M} S_{pp} \int_{f, g} h_{L M}^{j_1 M} i h_{j_1 2}^{j_2 M} S_{pp} \int_{f, g} h_{L M}^{j_1 M} i \\
 &Y_{L M}^{j_1 M}(\hat{p}_{rel}) Y_{L M}^{j_2 M}(\hat{p}) Y_{L M}^{j_3 M}(\hat{p}) \\
 &\exp(i q r) R_{j_1 2}^{j_2}(\mathbf{r}) R_{j_1 2}^{j_2}(\mathbf{r}) (i)^{j_1} I_{f, g}^{p_{rel}, j}(j); \quad (22)
 \end{aligned}$$

where f, g denotes the full set of quantum numbers characterizing the ground-state partial configurations in the ^3He wave function, and $I_{f, g}^{p_{rel}, j}(j)$ are the corresponding overlaps with the scattering state wave functions.

In what follows the so-called symmetric (sym) kinematics [21]

$$p_n = 0; \quad p_1 + p_2 = q$$

will be considered, which corresponds, in PWA, to a ground-state configuration characterized by the two protons with equal and opposite momenta and the neutron with zero momentum. In the sym kinematics, the transition form factor $M^{(pp)}(p_n; p_{rel}; q)$, when interacts with proton "1" ("2"), will only depend upon $p_{rel} = q = 2 p_{2(1)}$, i.e., for a fixed value of $|j|$, will only depend upon $|p_{2(1)}|$ and the angle between q and $p_{2(1)}$. In PWA, when the angular momentum of the neutron is zero, also the pp pair has relative angular momentum zero, so that the cross section is almost entirely determined by the square of the 1S_0 component of the three-body wave function ($k_{rel}; k_n = 0$), which is shown in Fig.3.

The calculated transition form factor is shown in Fig.4. Calculations have been performed with three-body wave function obtained in ref. [19] using the AV18 interaction [22]. Our results, which are in agreement with the ones of Ref. [21] (where a different ground-state wave functions has been used), show that the pp rescattering is very large and completely distorts the PWA results.

In order to investigate to what extent FSI depend upon the kinematics of the process, we have also considered the super-parallel (s.p.) kinematics, according to which one still has $p_n = 0, p_1 + p_2 = q$, but all momenta are collinear, i.e. ($q \parallel k_z$)

$$p_{1z} = p_{2z} = 0 \quad p_{1z} + p_{2z} = |q| \quad (23)$$

The results of calculations, which are presented in Fig.5, look very different from the ones shown in Fig. 4. Concerning these differences, the following remarks are in order:

1. as far as the PWA results are concerned, it can be seen that the transition matrix elements differ, at the same value of θ , by more than one order of magnitude; the reason is that the relative momentum k_{rel} at a given value of θ , is very different in the two kinematics, with $k_{rel}^{(sym)} \neq k_{rel}^{(sp)}$ (e.g. at $\theta = 0.2$ GeV one has $k_{rel}^{(sp)} \approx 0.45 \text{ fm}^{-1}$, whereas $k_{rel}^{(sym)} \approx 2.2 \text{ fm}^{-1}$). Since in both kinematics $M^{PWA}(k_n; k_{rel})$ is entirely determined by the 1S_0 three body wave function ($k_{rel} \cdot k_n = 0$), the value of θ at which this exhibits its minimum is different in the two cases;
2. in Fig. 4 the pp rescattering effects depend upon the value of the relative momentum of the two protons in the final state $p_{rel} = p_1 \sin \frac{12}{2} \neq k_{rel}$. Unlike the PWA case, one has $p_{rel}^{(sym)} \neq p_{rel}^{(sp)}$ (e.g. at $\theta = 0.2$ GeV one has $|p_1| \approx 535 \text{ MeV}/c$, $|p_2| \approx 0.45 \text{ fm}^{-1}$ and $|p_{rel}| \approx 1.8 \text{ fm}^{-1}$, in the sp. kinematics, and $|p_1| = |p_2| \approx 2.2 \text{ fm}^{-1}$, $\theta \approx 105^\circ$ and $|p_{rel}| = |p_1| \sin \frac{12}{2} \approx 1.7 \text{ fm}^{-1}$ in the sym kinematics). Thus, the two-proton relative energy in the final state is larger in the sp. kinematics, which explains the apparent smaller effects of FSI in Fig. 5. In this respect, it should however be pointed out that at values of $\theta > 0.7 - 0.8$ GeV, i.e. at large values of $p_{2z} \approx 1 \text{ fm}^{-1}$, where correlation effects are more relevant, the momentum transfer $|q|$ and the relative momentum of the proton pair become very large, and the Schrodinger equation can not in principle be applied to describe the pp-interaction in the continuum (e.g. in the sp. kinematics, when $|q| \approx 1 \text{ GeV}/c$, $|p_2| \approx 0.5 \text{ GeV}/c$, $|p_1| \approx 1.5 \text{ GeV}/c$, $|p_{rel}| \approx 1 \text{ GeV}/c$). To treat the case of high energies, a Glauber-type calculation is in progress and will be reported elsewhere [24]. Thus, it appears that in the sp. kinematics considered in Fig. 5, there exists only a small bin of $\theta \approx 0.4 - 0.5$ GeV where two-nucleon correlations could be investigated treating the pp rescattering within the Schrodinger equation;
3. recent preliminary experimental data from TNAF have been reported ([16, 17]), in which protons 1 and 2, with momenta higher than the Fermi momentum, are detected along (the forward proton) and against (the backward proton) the momentum transfer q within angles $\theta_{1q}, \theta_{2q} \approx 10^\circ$, with the momentum of the spectator neutron less than $\approx 0.76 \text{ fm}^{-1}$. The cross section, integrated over all variables implied by such a

kinematics, is presented vs the quantity

$$p_r = \frac{p_1 + q + p_2}{2} \quad (24)$$

which, provided FSI effects are absent ($p_1 = k_1 + q, p_2 = k_2$), is nothing but the relative momentum of the pp pair before interaction, $k_{rel} = (k_1 - k_2)/2$. The kinematics used in Fig. 5 is the limit ($p_n \rightarrow 0$) of the kinematics selected by the experiments, but the integral over p_{1q}, p_{2q} , and $p_n \rightarrow 0.76 \text{ fm}^{-1}$, will change the theoretical curves shown in Fig. 5 in several respects: first, unlike the case $p_n = 0$, besides the 1S_0 wave, all even waves of the relative motion contributes to the cross section, which means that not only the diffraction minimum will be washed out, but MEC and IC production may contribute to the process; secondly, the effects from FSI will also be different, for the super-parallel kinematics is violated. To sum up, a calculation including FSI as in Fig. 5 performed within the kinematical conditions of Ref. [16], [17] would be highly desirable. Calculations are in progress and will be reported elsewhere.

The next contribution to be considered is the proton-neutron rescattering (diagram (c) in Fig. 2). This has been found in Ref. [21] to provide very small effects, as also recently found in Ref. [18]. This point will be discussed in details in the next Section.

B. Process 2: absorption of π^+ by the neutron.

1. The Plane Wave Approximation and the pp rescattering

We will now consider the process $^3\text{H} e(e; e^0 p_1 p_2) n$, in which π^+ interacts with the neutron and the two protons are emitted and detected. We will consider two extreme cases of this process, viz: i) in the initial state the neutron is a partner of a correlated proton-neutron pair, with the second proton far apart from the pair; ii) in the initial state the neutron is at rest, far apart from the two correlated protons. Process i) has been considered in Ref. [6] for the case of both a neutron and a proton at rest in the initial state. We will compare our results with the ones of Ref. [6], considering only the case of the neutron at rest. The various mechanisms, in order of increasing complexity, which contribute to the above process, are depicted in Fig. 6.

When the final state rescattering between the two protons is taken into account (processes a) plus process b)), but the interaction of the hit neutron with the emitted proton-proton

pair is disregarded, one has $p_n = k_n + q$, and the cross section (Eq. (4)) integrated over P and the kinetic energy of the neutron, has the following form

$$\frac{d^8}{d_e^0 d_e^0 d_{p_n} d_{p_{rel}} d_{p_{rel}}} = K(Q^2; p_n; p_{rel}) R(Q^2; p_n; p_{rel}) \quad (25)$$

with

$$R_L(Q^2; p_n; p_{rel}) = G_E^n(Q^2)^2 M^{(pp)}(p_n; p_{rel}; q) \quad (26)$$

where $G_E^n(Q^2)$ is the neutron electric form factor, K incorporates all kinematical variables, and $M^{(pp)}(p_n; p_{rel}; q)$ is the transition nuclear form factor which, besides the PWA contribution, includes also the rescattering between the two spectator protons, viz

$$M^{(pp)}(k_n; p_{rel}) = \frac{1}{2} \sum_{M, S_{pp}; pp, n} \int T^{pp}(M; n; S_{pp}; pp; k_n; p_{rel})^2 \quad (27)$$

with T^{pp} having the following form

$$T^{pp}(M; n; S_{pp}; pp; k_n; p_{rel}) = \int d^3 r \exp(i k_n \cdot r) \frac{1}{2} \int_n I_M^{t, pp}(S_{pp}; pp) \quad (28)$$

where $k_n = p_n - q = (p_1 + p_2)$, and I^t is the overlap integral between the three-nucleon ground-state wave function and the two-proton continuum state, i.e.

$$I_M^{t, pp}(S_{pp}; pp) = \int d^3 r \frac{1}{2} \int_n I_M^t(S_{pp}; pp)(r) \frac{1}{2} M(r;) d^3 r \quad (29)$$

It should be stressed here that in the process analyzed in the previous Section, the pp rescattering was between the protons of the active pair which absorbed the virtual photon, whereas in this case is absorbed by the neutron and the pp rescattering involves the two spectator protons.

Within the PWA, i.e. when only process a) contributes to the reaction, one has

$$I_{S_{pp}; pp}^t(r) = I_{S_{pp}; pp}^t \exp(i r \cdot r) \text{ so that}$$

$$I_{N_2 N_3}^{t, PWA}(\) = \int d^3 r \frac{1}{2} M(r;) I_{S_{pp}; pp}^t \exp(i r \cdot r) d^3 r \quad (30)$$

and

$$\frac{T}{Z}^{PW A} (M ; n ; S_{pp} ; p_p ; k_n ; k_{rel}) = \int d^3 r d^3 r' \frac{1}{2} M (r ;) \frac{1}{2} n \exp (i k_n \cdot r) S_{pp} ; p_p \exp (i k_{rel} \cdot r') ; \quad (31)$$

is, as in Process 1), nothing but the three-nucleon wave function in momentum space.

It is interesting to point out that the integral of the transition form factor (27) over the direction of p_{rel} , is related to the neutron Spectral Function $P_1(k_n ; E)$ ([23])

$$P_1(k_n ; E) = \frac{1}{(2\pi)^4} \int d^3 p_{rel} \int d^3 r d^3 r' \exp (i k_n \cdot r) \frac{1}{2} n S_{pp} ; p_p (r) \frac{1}{2} M (r ;)^2 \quad (32)$$

by the following relation

$$\int d^3 p_{rel} P_1(k_n ; p_{rel}) = P_1(k_n ; E) \quad (33)$$

where

$$P_1(k_n ; p_{rel}) = \frac{M_N}{2} \int d^3 p_{rel} M^{pp}(k_n ; p_{rel}) \quad (34)$$

will be called here the Vector Spectral Function and

$$E = \frac{p_{rel}^2}{M} = \frac{(p_1 - p_2)^2}{4M} \quad (35)$$

is the "excitation energy" of the spectator pp pair, which is related to the removal energy E of the neutron by the relation $E = E_3 + E$, where E_3 is the (positive) binding energy of the three-nucleon system (cf Ref. [23]).

The cross section for the $^3H e(e;e^0 p_1 p_2)n$ can then be written in the following form

$$\frac{d^8}{d_e^0 d_{e^0} d_{p_n} d_{p_{rel}} d_{p_{rel}}} = K Q^2 ; p_n ; p_{rel} \frac{G_E^n(Q^2)}{M_N \int d^3 p_{rel}} P_1(k_n ; p_{rel}) \quad (36)$$

Note that the cross section (36) integrated over p_{rel} , provides the cross section for the semi-inclusive process $^3H e(e;e^0 n)pp$

$$\frac{d^6}{d_e^0 d_{e^0} d_n d_{p_{rel}}} = K G_E^n(Q^2)^2 P(k_n ; E) \quad (37)$$

The neutron Spectral Function calculated with and without the pp rescattering [23] is shown in Fig. 7. It can be seen that at $k_n \approx 1.5 \text{ fm}^{-1}$ there are regions, peaked at $E \approx \frac{k_n^2}{4M}$,

where the pp rescattering does not play any role; since $E = \frac{p_{rel}^2}{M}$, at the peaks we have the following relation between k_n and p_{rel}

$$k_n = 2p_{rel} \quad (38)$$

The positions of the peaks have been originally interpreted as arising from a two-nucleon correlation (2N C) configuration, where proton "1(2)" is correlated with the neutron with momenta satisfying the following relations: $k_{2(1)} = 0, k_{1(2)} = k_n$ [26]; moreover, the energy dependence around the peaks can be related to the motion of the third particle $k_{2(1)} \neq 0$, or, equivalently, to the Center-of-Mass motion of the correlated pair [27]. The existence of the region where pp rescattering is vanishing, is a general feature of any Spectral Function, independently of the two-nucleon interaction and the method to generate the wave function. This is illustrated in Fig. 4 where the Spectral Function corresponding to the variational three-body wave function of Ref. [19] obtained with the the AV18 interaction [22], is shown for several values of $k = k_n$. It can be seen that for values of k_n which satisfy relation (38), FSI effects generated by pp rescattering are negligible.

Relation (38) does not necessarily implies a 2N C configuration, i.e. $k_{2(1)} = 0, k_{1(2)} = k_n$, for it holds also if $k_{2(1)} \neq 0, k_{1(2)} = k_n$. The analysis of the Vector Spectral Function $P_1(k_n; p_{rel})$ should tell us what are the dominant configurations in the three-body wave function. To this end, we have plotted the Vector Spectral Function vs k_n in correspondence of two values of p_{rel} , viz $p_{rel} = 0.75 \text{ fm}^{-1}$ ($E = p_{rel}^2/M = 23 \text{ MeV}$) and $p_{rel} = 1.1 \text{ fm}^{-1}$ ($E = p_{rel}^2/M = 50 \text{ MeV}$) and various values of k_n . The results, which are shown in Fig. 9, deserve the following comments:

1. the constant behaviour of P_1 at $k_n = 0$ can easily be understood by considering that, as previously discussed, only the angle independent 1S_0 pp wave function contributes;
2. eq. (38), i.e. the relation $k_n = 2p_{rel}$ would correspond to $k_n = 1.5 \text{ fm}^{-1}$, when $p_{rel} = 0.75 \text{ fm}^{-1}$, and to $k_n = 2.2 \text{ fm}^{-1}$, when $p_{rel} = 1.1 \text{ fm}^{-1}$. It can be seen that when $k_n = 2p_{rel}$ pp rescattering effects almost disappear, but they become extremely large when such a relation is not satisfied, except when $k_n = 2p_{rel}$ and $\theta = 0; 180^\circ$;

3. when $k_n = 2p_{rel}$ the value $\theta = 0^\circ (180^\circ)$ (super-parallel kinematics), corresponds to $k_{1(2)} \neq 0, k_n = k_{2(1)}$, i.e. to the 2N C configuration (see Appendix 2). The results presented in Fig. 9 clearly show that such a configuration is the dominant one; as a matter of fact, far from such a configuration (e.g. at $\theta = 90^\circ$, when three-nucleon configurations are important), the Vector Spectral Function is sensibly smaller. Thus, the most probable configuration in the three-nucleon wave function, when $k_n = 2p_{rel}$ is indeed the 2N C configuration, when one nucleon of the pp pair is almost at rest and the second one has momentum almost equal and opposite to the momentum of the neutron;
4. when $k_n \neq 2p_{rel}$ we still stay in the super-parallel kinematics but not in the two-nucleon correlation region, for now $k_{2(1)} \neq 0, k_n \neq k_{1(2)}$; however, it can be seen that for $k_n > 2p_{rel}$ and $\theta \neq 0^\circ; 180^\circ$, when the violation of the condition $k_n = 2p_{rel}$ is very mild, pp rescattering effects are still very small; note, moreover, that if the FSI can only be described by the pp rescattering, the cross section should be the same at both angles, a behaviour which deserves experimental investigation.

Thus the study of the Vector Spectral Function at $k_n = 2p_{rel}, \theta = 0^\circ$ or 180° , which could be undertaken by measuring the $(e;e^02p)$ process in the super-parallel kinematics, would allow one to obtain information on the three-nucleon wave function in momentum space, provided the rescattering of the two protons with the outgoing neutron does not appreciably distort the process. The full calculation of the transition matrix element has been undertaken in Ref. [6] within a consistent Faddeev approach to bound and continuum states of the three-nucleon system. The process considered in Ref. [6] is the absorption of a neutron (proton) at rest with the two protons (proton-neutron) emitted back-to-back with equal momenta $p_1 = p_2 = p$ and the neutron with momentum $p_n = q$ emitted in a direction perpendicular to p . This is our Process 2) discussed in Section II. We will present the calculation of this process within an approximate treatment of the n pp rescattering based upon the eikonal approximation, which not only could easily be extended to complex nuclei, but could also be applied at high np relative energies when the Schrodinger approach cannot be applied. For sake of comparison we will consider the case of the neutron at rest, since in Ref. [6] rescattering effects in this case have been found to be very large.

C . The three-body rescattering

We have considered the three-body rescattering of the neutron with the interacting pp pair within an extended Glauber-type approach [28] based on the following replacement

$$\frac{1}{2} \int d^3r_3 \exp(i\mathbf{p}_n \cdot \mathbf{r}_3) P_{S_{pp} \text{ pp}}^{\text{rel}}(\mathbf{r}_1; \mathbf{r}_2) \rightarrow \hat{G}(\mathbf{r}_1; \mathbf{r}_2; \mathbf{r}_3) \frac{1}{2} \int d^3r_3 \exp(i\mathbf{p}_n \cdot \mathbf{r}_3) P_{S_{pp} \text{ pp}}^{\text{rel}}(\mathbf{r}_1; \mathbf{r}_2) \quad (39)$$

where the Glauber operator \hat{G} is [29]

$$\hat{G}(\mathbf{r}_1; \mathbf{r}_2; \mathbf{r}_3) = \prod_{i=1}^3 [1 - (z_i - z_0) b_i]; \quad (40)$$

with b_i and z_i being the transverse and the longitudinal co-ordinates of the nucleon, and b_i the profile function of the elastic nucleon-nucleon scattering amplitude; for the latter, the standard high-energy parametrization viz,

$$b_i = \frac{\sigma_{NN}^{\text{tot}} (1 - i \alpha_{NN})}{4 b_0^2} \exp\left(-\frac{b_i^2}{2b_0^2}\right) \quad (41)$$

has been used, where σ_{NN}^{tot} is the total Nucleon-Nucleon (NN) cross section, α_{NN} the ratio of the imaginary to the real part of the NN scattering amplitude. Within such an approach, the full distorted transition matrix element assumes the following form

$$T^D(\mathbf{p}_m; \mathbf{p}_{\text{rel}}) = \frac{1}{2} \sum_{M, S_{pp}; pp} \sum_{n} \int T^D(M; n; S_{pp}; pp; \mathbf{p}_m; \mathbf{p}_{\text{rel}}) \quad (42)$$

where

$$\mathbf{p}_m = \mathbf{p}_n \quad \mathbf{q} = (\mathbf{q} + \mathbf{p}_2) \quad (43)$$

is the missing momentum, which coincides with the neutron momentum before interaction when the three-body rescattering is disregarded. The distorted scattering matrix T^D has the form

$$T^D(M; n; S_{pp}; pp; \mathbf{p}_n; \mathbf{p}_{\text{rel}}) = \frac{2}{\pi} \int_0^Z \int d^2t d^3r \exp(i\mathbf{p}_m \cdot \mathbf{r}) T_{M; n; S_{pp}; pp}^{\text{rel}}(\mathbf{r}; \mathbf{r}); \quad (44)$$

with

$$T_{M; n; S_{pp}; pp}^{\text{rel}}(\mathbf{r}; \mathbf{r}) = \sum_{f, g} \sum_{h, l, m} \sum_{j_1, j_2} \frac{1}{2} \int d^3r_1 d^3r_2 \int d^3r_3 \exp(i\mathbf{p}_n \cdot \mathbf{r}_1 + i\mathbf{p}_{\text{rel}} \cdot \mathbf{r}_2) Y_{l, m}^{j_1}(\hat{\mathbf{r}}_1) Y_{l, m}^{j_2}(\hat{\mathbf{r}}_2) R_{l, S_{pp}}^{j_1; t}(\mathbf{r}) R_{l, S_{pp}}^{j_2; t}(\mathbf{r}) Y_{l_2, S}^{j_1, j_2}(\hat{\mathbf{r}}) Y_{l, S}^{j_1, j_2}(\hat{\mathbf{r}}) \hat{G}(\mathbf{r}; \mathbf{r}); \quad (45)$$

Within such an approach, the cross section is represented by Eq. (25), with $M^{pp}(p_n; p_{rel})$ replaced by $M^D(p_n; p_{rel})$ [30].

Here some details of our numerical calculations of the three-body rescattering transition form factors are in order. As it can be seen from eqs.(44) and (45), the dependence of $T^D(M; n; S_{pp}; pp; p_n; p_{rel})$ upon p_{rel} is entirely governed by the quantity ${}^{t\bar{t}}M; n; S_{pp}; pp(r;)$. Since the main component of the 3H_e ground-state wave function corresponds to the relative motion of the pp pair in the 1S_0 wave, the two protons in the final state are mostly in states with spin $S = 0$ and even values of the relative angular momentum; thus ${}^{t\bar{t}}M; n; S_{pp}; pp(r;)$ is almost symmetric under the exchange $t \leftrightarrow \bar{t}$. This symmetry can be slightly violated due to the contribution of the highest partial pp-waves in the 3H_e wave function [29].

The quantities $\frac{N N}{N N}$, $N N$ and b_0 in eq. (41) depend in principle on the total energy of the interacting nucleons [28], however at high values of p_n ($p_n \approx 0.7 GeV/c$, which implies high values of the momentum transfer q), they become energy independent and the "asymptotic" values $\sigma_{tot}(NN) \approx 44 mb$, $\frac{N N}{N N} \approx 0.4$ can be used, with b_0 determined by $\frac{N N}{N N}$ and $N N$ from unitarity requirements [28].

The transition form factor $M^D(p_n; p_{rel})$ is shown Figs.10, 11 and 12 where it is compared with $M^{PW A}$ and M^{pp} . The three Figures correspond to three different kinematical conditions, namely:

1. Fig. 10 shows the results obtained in the super-parallel kinematics ($\theta_1 = 180^\circ$) and $p_{rel} = 0.75 fm^{-1}$, vs $q = p_1 + p_2 = p_n - q$. Let us discuss the results within the PW A and the pp rescattering contribution (dashed and dot-dashed curves). In this case, $p_n = k_n + q$ and $P = p_{mis} = k_n$, and we get the results presented in Fig. 9 (top panel) at $\theta_1 = 180^\circ$; the arrow denotes the 2N C kinematics, when $k_1 = k_n$, $k_2 = 0$ ($p_1 + p_n = q$, $p_2 = 0$) and $q = 2p_{rel}$. In agreement with Fig. 9, we see that the pp rescattering has large effects at low values of $q = q$ but gives negligible contributions when $q = q - 2p_{rel} = 1.5 fm^{-1}$. As for the effects of the n pp rescattering (when $p_m \neq k_n$), they are very large at small values of q but become negligible at $q = 2p_{rel}$. One could be tempted to compare the results shown in Fig. 10 with the ones shown in Fig. 5. In this respect one should first of all stress that in the symmetric kinematics shown in Fig. 5, the neutron is at rest (both in the initial and final states), which means that the transition matrix element is mainly governed by the

1S_0 wave function of the two-proton relative motion. In the process considered in Fig. 10, when γ couples to the neutron, none of the nucleons are at rest, except nucleon "2" in the particular kinematics denoted by the arrow which represents the absorption of γ by a neutron of a correlated np pair, with the spectator proton at rest both in the initial and the final states. In this case, other angular momentum states, besides the 1S_0 one, contribute to the transition matrix element, with the result that there no diffraction minimum appears; thus, in principle, there is no relationship between the two Figures. Nonetheless, one should expect that the other angular momentum states should produce only a minor effect left and right to the diffraction minimum of the 1S_0 , so that, in these regions, the value of $M(\mathbf{P}; \mathbf{p}_{rel}; j_1)$ corresponding to the arrow in Fig. 10 can qualitatively be compared with the results shown in Fig. 5, taking there $p_{2z} = -p_{1z} = 1.5 \text{ fm}^{-1}$; in this case one finds indeed that the relative momentum of the np pair is $|\mathbf{p}_{rel}| = 0.75 \text{ fm}^{-1}$. Thus, in Fig. 5 the region where FSI effects are small, correspond to the 2N C region; moreover, there, the conditions for the validity of the Schrodinger approach hold. Note, eventually, that, according to our Glauber calculation, as well as to the calculation of Ref. [21], the curve shown in Fig. 5 are slightly affected by the pn rescattering; thus the dashed line in Fig. 5 includes effectively both the PWA and pp rescattering results shown in Fig. 10.

2. Fig. 11 displays the same as in Fig. 10, but for $\theta_1 = 90^\circ$. The dashed and dot-dashed lines are the same as in Fig. 9. In particular, at $|\mathbf{k}_n| = 1.5 \text{ fm}^{-1}$, corresponding to the condition $|\mathbf{k}_n| = 2|\mathbf{p}_{rel}|$ the n pp rescattering is small. Note that in this case, in spite of the fulfillment of the above condition, we are not in the two-nucleon correlation region but rather in the three-nucleon correlation region, for, as shown in the Figure, the momenta of the three nucleons in the ground-state are of comparable size ($|\mathbf{k}_1|, |\mathbf{k}_2|, |\mathbf{k}_n| \approx \frac{p}{2}$, $\theta_{12} \approx 90^\circ$). Note that in the PWA the transition form factor both in Process 1 (interaction of γ with a proton of a correlated pp pair shown in Figs. 4 and 5) and Process 2 (the interaction of γ with the neutron we are discussing), represent the same quantity, namely the three-body wave function in momentum space (cf. Eqs. 15 and 31); therefore the results presented in Figs. 10 and 11 at $|\mathbf{P}| = |\mathbf{k}_n| = 0$ have to coincide with the ones given in Fig. 3 at the corresponding value of $p_{rel} = k_{rel}$, as indeed is the case;

3. Fig. 12 refers to the particular case when the neutron is at rest in the ground-state, so that, after absorbing γ , it leaves the system with momentum $p_n = q$, and the two protons are emitted back-to-back in the lab system with $|p_1| = |p_2|$ and $\theta_1 = 90^\circ$. This is the kinematics also considered in Ref. [6]. Since, as already pointed out (cf. Section 3.2.1, Eq. 31), in PWA both Process 1 and Process 2 are described by the same transition form factor, which is nothing but the momentum space three-body wave function, the dashed lines in Figs. 4 and 12 represent the same quantity. As a matter of fact, since in Fig. 12 $|p_{rel}| = |p_2|$, we see that at the highest values of $|p_{rel}|$ the dashed lines in Fig. 4 and 12 are in agreement; note, however, that due to the effect of the angular momentum states, the dashed line in Fig. 12 should not exhibit the diffraction minimum seen in Fig. 4. It can be seen, as expected from the behaviour of the neutron spectral function, that the pp rescattering is very large since the ground-state configuration corresponds to zero neutron momentum and large pp relative momentum. The fact that the pp rescattering is large, would not represent per se a serious obstacle in the investigation of the three-body spectral function, for, as also stressed in Ref. [6], the calculation of the pp rescattering is well under control since many years (see e.g. Ref. [23]); unfortunately, also the full rescattering effects are very large, with the results that this kinematics is not the optimal one to investigate the three body wave function. As for the comparison with the Faddeev results of Ref. [6], our PWA and pp rescattering results agree with the ones (PWA IAS and "G₀", respectively) obtained in Ref. [6]; as far as the three-body rescattering contribution is concerned, there also appear to be a satisfactory agreement between our Glauber-type calculation and the Faddeev results, provided the values of the three-momentum transfer is large enough; at low values of the momentum transfer the Glauber-type approach cannot be applied and a consistent treatment of bound and continuum three-nucleon states within the Schrodinger approach is necessary. In Ref. [6] the effect of the three body rescattering on the process in which γ is absorbed by a proton at rest and the proton and the neutron are emitted back-to-back with equal momenta $p_n = p_2 = p$, and the proton emitted with momentum $p_1 = q$ has, on the contrary been found to be very small, so that this process would be suited for the investigation of the three-nucleon wave function, being the calculation of the p-p(n) rescattering well under control, as already pointed out. However, the s.p. kinematics

at $\mathbf{j} = 2\mathbf{j}_{rel}$ we have considered seems to be very interesting, due to the apparent lack of FSI effects.

IV. SUMMARY AND CONCLUSIONS

In this paper we have investigated the effects of the Final State Interaction (FSI) in the process ${}^3\text{H} e(e; e^0 p_1 p_2) n$, using realistic three-nucleon wave functions which, being the exact solution of the Schrodinger equation, incorporate all types of correlations generated by modern NN potentials. Basically we have considered two different mechanisms leading to the two-proton emission process:

1. Mechanism 1, in which ${}^3\text{H}$ is absorbed by a correlated pp pair. This mechanism, which is the one usually considered in the case of complex nuclei, has been previously analyzed in Ref. [21] within a particular kinematics, the so called symmetric kinematics, according to which $\mathbf{p}_1 + \mathbf{p}_2 = \mathbf{q}$, $\mathbf{p}_n = 0$. In PWA, such a kinematics selects the ground-state wave function configuration in which $k_1 = k_2$, $k_n = 0$ (the two-nucleon correlation (2N C) configuration). Our calculations confirm the results of Ref. [21], namely that the FSI due to the n (pp) rescattering is very small, whereas the pp rescattering is extremely large, and fully distorts the direct link between the ground-state wave function and the cross section, which holds in PWA (cf. Fig. 4). Thus, the symmetric kinematics does not appear extremely useful to investigate the three-nucleon wave function. A more interesting kinematics is the super-parallel kinematics ($p_{1z} = p_{2z} = 0; p_{1z} + p_{2z} = \mathbf{j} \cdot \mathbf{j} / q k z$) which, as demonstrated in Fig. 5, shows that, particularly at high values of the momenta of the detected protons, the effects from the FSI are strongly reduced;
2. Mechanism 2, in which ${}^3\text{H}$ is absorbed by the neutron, and the two protons are detected. We have shown that if the pp rescattering is taken into account and the one between the neutron and the protons disregarded, the cross section depends upon the Vector Spectral Function $P_1(\mathbf{k}_n; \mathbf{p}_{rel}) = \frac{M_N \mathbf{p}_{rel}}{2} M^{pp}(\mathbf{k}_n; \mathbf{p}_{rel})$. This Spectral Function, unlike the usual one (see e.g Ref. [23]), depends not only upon $|\mathbf{k}_n|$ and $|\mathbf{p}_{rel}| = \frac{p}{2ME}$, but also upon the angle θ between them. By analyzing the behaviour of $P_1(\mathbf{k}_n; \mathbf{p}_{rel})$ (cf. Fig. 9) we have demonstrated that: i) when the relation

$k_n \approx 2p_{rel}$ holds, the FSI due to pp rescattering is very small, and ii) the dominant configuration in the ground-state wave function is the 2N C one, in which $k_1 \approx k_2$, $k_n = 0$ (Eq. 34); we have also found that when $\theta \approx 0^\circ$ (180°), the smallness of pp rescattering actually extends to a wide region characterized by $k_n \approx 2p_{rel}$ where the 2N C configuration is still the dominant one (cf. Appendix 2). Such a picture is not in principle withstanding when the three-nucleon n (pp) rescattering is taken into account, since in this case the concept of neutron momentum before interaction k_n has to be abandoned in favor of the concept of missing momentum $p_m = p_n - q = -(p_1 + p_2)$, which equals k_n only when the three-body rescattering is disregarded. However, our consideration of the three-body rescattering, clearly show that in the case of the super-parallel kinematics both the three-body and two-body rescattering are negligible when $p_m \approx 2p_{rel}$ which means that in this region $p_m \approx k_n$. The three-body rescattering is on the contrary very relevant when $p_m \approx 2p_{rel}$, both in the case of the super-parallel kinematics, and particularly when the two protons are detected with their relative momentum perpendicular to the direction of q (cf. Fig. 11). Within Mechanism 2 we have, as in Ref. [6], also considered the process in which n is absorbed by a neutron at rest and the two protons are emitted back-to-back in the direction perpendicular to the direction of the momentum transfer q , which means $p_m = 0$. In this case, the effects from the FSI appear to be very different from the ones considered in the two previous cases, namely, unlike the symmetric kinematics (cf. Figs. 4 and 5), where only the FSI between the two active protons played a substantial role, here both the pp rescattering and the three-body n (pp) rescattering are very large (cf. Fig. 12).

We can summarize the main results we have obtained in the following way:

i) if n is absorbed by a correlated proton pair, with the spectator neutron at rest and the two protons detected with their relative momentum perpendicular to the direction of q (symmetric kinematics), the leading FSI is the pp rescattering, with the n (pp) rescattering playing only a minor role. In such a case, however, the pp rescattering fully destroys the direct link between the ground-state wave function and the cross section, occurring in the PWA; if the protons, on the contrary, are detected with their relative momentum parallel to q (super-parallel kinematics), the effects of the pp rescattering is appreciably suppressed, particularly at high values of the momenta of the detected protons;

ii) if α is absorbed by an uncorrelated neutron at rest and the two correlated protons are emitted back-to-back with $p_1 = -p_2, p_{rel} = p_1 + q$, both the pp and the n (pp) rescattering are very large;

iii) if α is absorbed by a neutron and the two protons are detected in the super-parallel kinematics, one has the following situation: if $p_m \ll 2p_{rel}$ both the pp and the n (pp) rescattering are large; if, on the contrary, $p_m \sim 2p_{rel}$ they are both small and the cross section can be directly linked to the three-body wave function in momentum space.

In conclusion it appears that the super-parallel kinematics with $p_m \sim 2p_{rel}$ could represent a powerful tool to investigate the structure of the three-body wave function in momentum space.

Acknowledgments

This work was partially supported by the Ministero dell'Istruzione, Università e Ricerca (MIUR), through the funds COFIN 01. We are indebted to A. Kievsy for making available the variational three-body wave functions of the Pisa Group and to W. Glockle for useful discussions and for supplying the results of the $^3\text{He}(e;e^0pp)n$ calculations prior to publications. We thank L. Weinstein and B. Zhang for the information they provided on the CLAS preliminary results on two-proton emission of ^3He . L.P.K. is indebted to the University of Perugia and INFN, Sezione di Perugia, for warm hospitality and financial support.

[1] W. Glockle et al, Phys. Rep. 274 (1996) 107.

[2] J. Carlson and R. Schiavilla, Rev. Mod. Phys. 70 (1998) 743.

[3] S.C. Pieper and R.B. Wiringa, Rev. Mod. Phys. 51 (2001) 53.

[4] S. Bo, C. Giusti and F.D. Pacati, Phys. Rep. 226 (1993) 1.

[5] S. Ishikawa et al, Phys. Rev. C 57 (1998) 29.

[6] W. Glockle et al in 5th Workshop on Electromagnetically Induced Two-Hadron Emission, Lund, Sweden, June 2001, Edited by P. Grabmayr; nucl-th/0109070, and Private communication.

[7] A. Kievsy, S. Rosati and M. Viviani, Nucl. Phys. A 551 (1993) 241

[8] C. Giusti and F.D. Pacati, Nucl. Phys. A 535 (1991) 573.

[9] T. Emura et al, Phys. Rev. Lett 73 (1994) 404.

- [10] P. Grabmayr, in *Proceedings of the Third International Conference on Perspectives in Hadronic Physics*, edited by S. Bo, C. Cio degli Atti and M. Giannini, Nucl. Phys. A 699 (2002) 41c.
- [11] C. Giusti and F. D. Pacati, Phys. Rev. C 57 (1998) 1691.
- [12] J. Ryckebusch et al, Nucl. Phys. A 624 (1997) 581. G. Rosner, in *Proceedings of the Conference on Perspectives in Hadronic Physics*, edited by S. Bo, C. Cio degli Atti and M. Giannini (ICTP, World Scientific, Singapore, 1997), p. 185.
- [13] C. Onderwater et al, Phys. Rev. Lett 78 (1997) 4893.
- [14] L. J. H. M. Kester et al, Phys. Lett. B 344 (1995) 79.
- [15] D. Groep et al. Phys. Rev. Lett. 83 (1999) 5444.
- [16] B. Zhang, W. Bertozzi and S. Gilad, in *5th Workshop on Electromagnetically Induced Two-Hadron Emission*, Lund, Sweden, June 2001, Edited by P. Grabmayr and Private communication.
- [17] L. B. Weinstein, in *5th Workshop on Electromagnetically Induced Two-Hadron Emission*, Lund, Sweden, June 2001, Edited by P. Grabmayr and Private communication.
- [18] C. Cio degli Atti and L. P. Kaptari, in *5th Workshop on Electromagnetically Induced Two-Hadron Emission*, Lund, Sweden, June 2001, Edited by P. Grabmayr;
C. Cio degli Atti and L. P. Kaptari in *Proceedings of the Third International Conference on Perspectives in Hadronic Physics*, edited by S. Bo, C. Cio degli Atti and M. Giannini, Nucl. Phys. A 699 (2002) 49c.
- [19] A. Kisevsky, S. Rosati and M. Viviani, Phys. Rev. Lett. 82 (1999) 3759;
A. Kisevsky, Private communication.
- [20] A. G. Sitenko, *Scattering Theory*, Springer-Verlag, Berlin-Heidelberg, 1991.
- [21] J. M. Laget, Phys. Rev. C 35 (1987) 832.
- [22] R. B. Wiringa, R. A. Smith and T. L. Ainsworth, Phys. Rev. C 29 (1984) 1207.
- [23] C. Cio degli Atti, E. Pace and G. Salmè in *Lecture Notes in Physics* 86 (1978) 315; Phys. Rev. 21 (1980) 805.
- [24] C. Cio degli Atti, L. P. Kaptari and H. Morita, to be published.
- [25] R. V. Reid Jr., Ann. Phys. 50 (1968) 411.
- [26] L. L. Frankfurt and M. I. Strikman, Phys. Rep. 160 (1988) 235.
- [27] C. Cio degli Atti, S. Simula, L. L. Frankfurt and M. I. Strikman, Phys. Rev. C 44 (1991)

R 7.

C. Cio degli Atti and S. Simula, Phys. Rev. C 53 (1996) 1689.

[28] C. Cio degli Atti, L. Kaptari and D. Treleani, Phys. Rev. C 63 (2001) 044601.

[29] A. Bianconi, S. Jeschonnek, N. N. Nikolaev, B. G. Zakharov Phys. Lett. B 343 (1995) 13.

[30] The quantity $P_1^D(k_n; p_{rel}) = M_N \dot{p}_{rel} M^D(k_n; p_{rel}) = 2$ can be called the Distorted Vector Spectral Function

APPENDIX

1. KINEMATICS OF THE PROCESS ${}^3\text{He}(e;e^0\text{pp})\text{n}$

The nucleon 4-momenta before interaction are denoted by k_i , and the ones after interaction by p_i . The energy-momentum conservation law in the Lab system reads as follows ($\hbar = c = 1$)

$$+ M_3 = E_1 + E_2 + E_n \quad (46)$$

$$p_1 + p_2 + p_n = q \quad (47)$$

$$(48)$$

and the invariant mass of the proton-proton pair is

$$s_{12} = (p_1 + p_2)^2 = (E_1 + E_2)^2 - q^2 = (M_3 + E_n)^2 - q^2 \quad (49)$$

where $M_3 = 3M_N = 7.7 \text{ MeV}$ is the mass of ${}^3\text{He}$, p_1, p_2 and p_n the momenta of protons "1" and "2" and the neutron, $E_i = \sqrt{M_N^2 + p_i^2}$ their total energy, q and the momentum and energy transfers.

Let us assume that in the process ${}^3\text{He}(e;e^0\text{pp})\text{n}$ the neutron is a spectator and the virtual photon is absorbed by one of the two protons; moreover, let us consider the symmetric kinematics when the neutron is at rest both in the initial and final states, i.e. $p_1 + p_2 = q$, $p_n = 0$. The relevant kinematical quantities in the Center-of-Mass (CM) system of the two protons (to be denoted by a superscript *), can be found (e.g. for proton "1") by the following Lorentz transformation ($\vec{p}_1^* = \vec{p}_2^* = \vec{p}_{\text{rel}}^*$, $E_1 = E_2 = E^* = \sqrt{p_{\text{rel}}^{*2} + M_N^2}$)

$$p_1 = p_1^* + \frac{V}{1 + V p_1^*} E_1^* \quad (50)$$

$$E_1 = E_1^* + V p_1^* \quad (51)$$

where

$$V = \frac{q}{E_1 + E_2} \quad (52)$$

$$= \frac{1}{1 - V^2} = \frac{E_1 + E_2}{\sqrt{s_{12}}} = \frac{M_3 + M_N}{\sqrt{s_{12}}} \quad (53)$$

$$V = \frac{q}{s_{12}} \quad (54)$$

and, by definition,

$$E = \frac{1}{2} \frac{p}{s_{12}} \quad \dot{p}_{rel} j = \frac{1}{2} \frac{q}{s_{12}} \sqrt{4M_N^2} : \quad (55)$$

Since $\dot{p}_{rel} j$ depends only upon q and θ , all quantities in the Lab system will depend upon q , θ , and $\phi_{p_{rel}}$, where the z-axis has been chosen along the direction of q . One obtains

$$\begin{aligned} p_{1z} &= \dot{p}_{rel} j \cos \theta_1 + \frac{1}{+1} (V)^2 \dot{p}_{rel} j \cos \theta_1 + \frac{1}{2} \dot{p} j \\ p_{1\phi} &= \dot{p}_{rel} j \sin \theta_1 \end{aligned} \quad (56)$$

and

$$\dot{p}_1 j = \frac{q}{p_{1z}^2 + p_{1\phi}^2} \quad (57)$$

The value of

$$\dot{p}_2 j = \frac{q}{p_{2z}^2 + p_{2\phi}^2} \quad (58)$$

is obtained by the replacement $\dot{p}_{rel} j \rightarrow \dot{p}_{rel} j$ in Eq. 56. The final state relative momentum in the Lab system, $p_{rel} = \frac{p_1 - p_2}{2}$, becomes a function of q , θ , and ϕ , which means that by varying ϕ , the relative momentum p_{rel} (its absolute value and its angle in the Lab system) varies correspondingly according to

$$p_{rel}^2 = \frac{1}{4} (p_{1z}^2 + p_{1\phi}^2 + p_{2z}^2 + p_{2\phi}^2) - \frac{q}{2} \frac{q}{p_{1z}^2 + p_{1\phi}^2} \frac{q}{p_{2z}^2 + p_{2\phi}^2} \cos \theta_{12} \quad (59)$$

where θ_{12} is the angle between p_1 and p_2 in the Lab. system, which can be obtained from the relation $(p_1 + p_2)^2 = q^2$, namely

$$\cos \theta_{12} = \frac{p_{1z} \dot{p} j - p_{1\phi} \dot{p}_2 j}{\dot{p}_1 j \dot{p}_2 j} \quad (60)$$

It can be seen from Eq. 56 that when $\theta_1 = 90^\circ$, $\dot{p}_1 j = \dot{p}_2 j = \frac{q}{4} (\frac{1}{+1} + M_3 - M_n)^2 - M_p^2$, $p_{1\phi} = p_{2\phi} = \dot{p}_{rel} j$ and $\theta_{12} = 2 \arccos \frac{\dot{p} j}{2 \dot{p}_2 j}$; when $\theta_1 = 0^\circ (180^\circ)$, $p_{2\phi} = p_{1\phi} = 0$, $\cos \theta_{12} = 1 (-1)$, and the final state momenta p_1 and p_2 are collinear with the momentum transfer q . Note, that because of the Pauli principle, in actual calculations one must either use explicitly antisymmetrization of the pair wave function, or perform all calculations for proton one at $0 < \phi_{p_{rel}} < 90^\circ$, bearing in mind that the second hemisphere in the phase space is occupied by the second proton. The results for $90^\circ < \phi_{p_{rel}} < 180^\circ$ may be obtained by mirror reflection of the results obtained for the first proton.

2. THE BASIC CONFIGURATIONS IN THE VECTOR SPECTRAL FUNCTION

Let us investigate the basic configuration in the Vector Spectral Function. To this end, we will first consider the three-body wave function in momentum space or, in other words, the Vector Spectral Function in the Plane Wave Approximation, when the momenta of the three nucleons satisfy the relation

$$k_1 + k_2 + k_n = 0 \quad (61)$$

ie.

$$k_{1(2)} = \frac{1}{2}k_n + k_{rel} \quad (62)$$

where $k_{rel} = \frac{k_1 - k_2}{2}$ is the relative momentum. One thus have

$$k_{1(2)}^2 = \frac{r}{k_{rel}^2 + \frac{k_n^2}{4}} k_{rel} k_n \cos \theta \quad (63)$$

The above relation illustrates that:

1. if $k_n^2 = 2k_{rel}^2$, $k_1^2 = 0$, $k_n = k_2$, when $\theta = 0^\circ$, and $k_2^2 = 0$, $k_n = k_1$, when $\theta = 180^\circ$, which represents the two-nucleon correlation (2N C) configuration. It should be pointed out that the scalar condition $k_n^2 = 2k_{rel}^2$ alone does not suffice to uniquely specify the ground-state configuration, in particular the 2N C configuration. As a matter of fact, when $k_n^2 = 2k_{rel}^2$ but $\theta = 90^\circ$, one has $k_1^2 = k_2^2 = \frac{p}{2}k_{rel}^2$ which represents a typical three-nucleon correlation (3N C) configuration, for all of the three nucleons have comparable and high momenta. However, it can be seen from Fig.9 that such a three-nucleon configuration is strongly suppressed, and $P(k_n; E)$ is mainly governed by the 2N C configuration.
2. If $k_n^2 \neq 2k_{rel}^2$, we do not stay in the 2N C configuration, but it can easily be checked that if $k_n^2 > 2k_{rel}^2$ and $\theta \neq 0^\circ (180^\circ)$, k_n^2 is still comparable with $k_{2(1)}^2 > k_{1(2)}^2$.

The above picture is distorted by the pp rescattering, but, as demonstrated in Fig. 9, only for: i) $k_n^2 < 2k_{rel}^2$ and ii) $k_n^2 > 2k_{rel}^2$, $\theta \neq 90^\circ$.

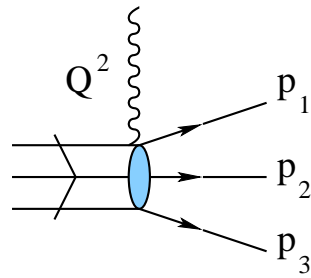


FIG. 1: The One Photon Exchange diagram for the two-nucleon (N) emission of ${}^3\text{He}$, ${}^3\text{He}(e;e^0N_1N_2)N_3$. Q^2 is the four-momentum transfer and p_i denotes the four-momentum of nucleon N_i in the final state. N_1 and N_2 denote the detected nucleons.

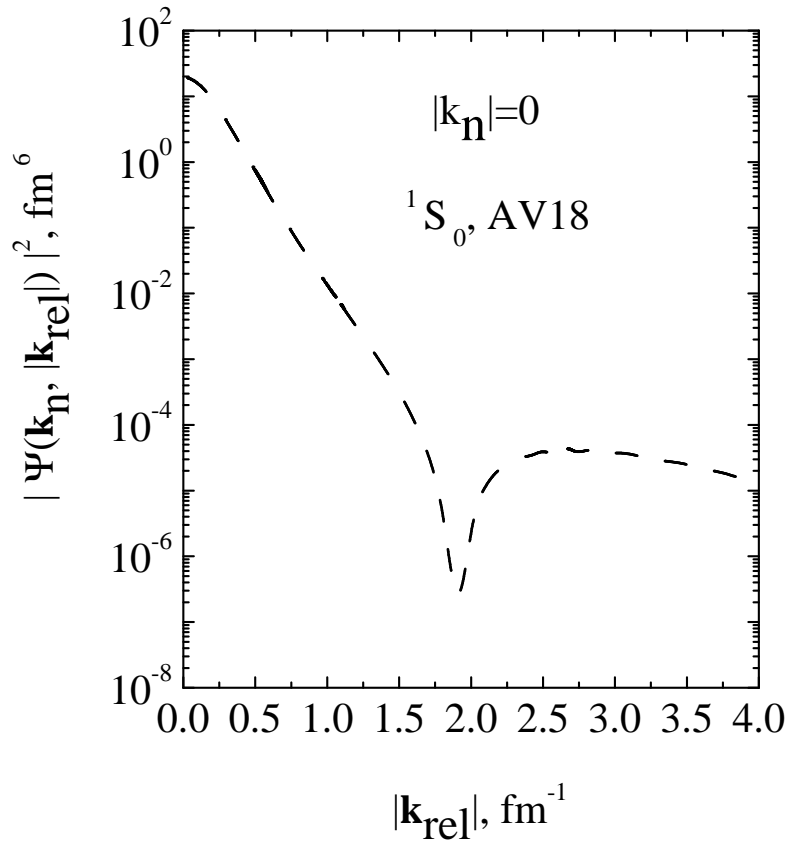


FIG. 3: The momentum space wave function of ^3He corresponding to the configuration in which the neutron is at rest and the two protons are in the state 1S_0 of relative motion with momentum $k_{\text{rel}} = (k_1 - k_2) = 2$. Three-body wave function from Ref. [19]; AV18 interaction [22].

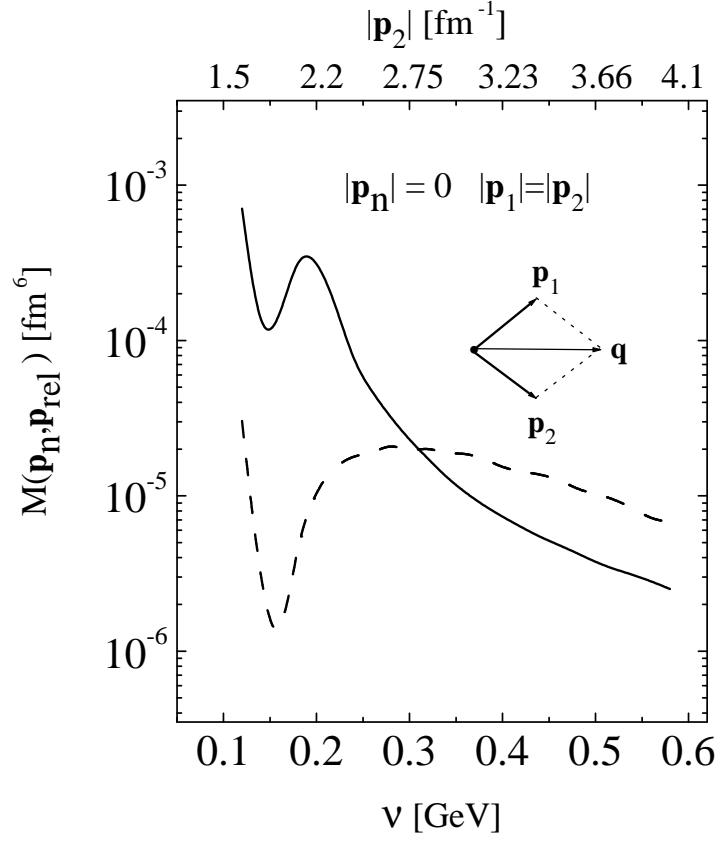


FIG. 4: The transition form factor $M(\mathbf{p}_n; \mathbf{p}_{rel}; \mathbf{q})$ (Eq.10) calculated in the Symmetric kinematics (21): $\mathbf{p}_1 + \mathbf{p}_2 = \mathbf{q}, \mathbf{p}_n = 0, |\mathbf{p}_1| = |\mathbf{p}_2| = \frac{q}{2}, p_{rel} = q = 2 p_2, \theta_{12} = 2 \arccos \frac{q}{2 p_2}$. The dashed line corresponds to the Plane Wave Approximation (PWA) (plane waves for the three nucleons, Process (a) in Fig. 2), whereas the full line includes the pp rescattering (Process (a) + Process (b) in Fig. 2). The value of q corresponds to $E_e = 2 \text{ GeV}$ and $\theta_e = 15^\circ$ (cf. Eq. 1), and the range of its variation with v is $0.52 \text{ GeV} = c q \leq q \leq 0.75 \text{ GeV} = c q$. Three-body wave function from Ref. [19]; AV18 interaction [22].

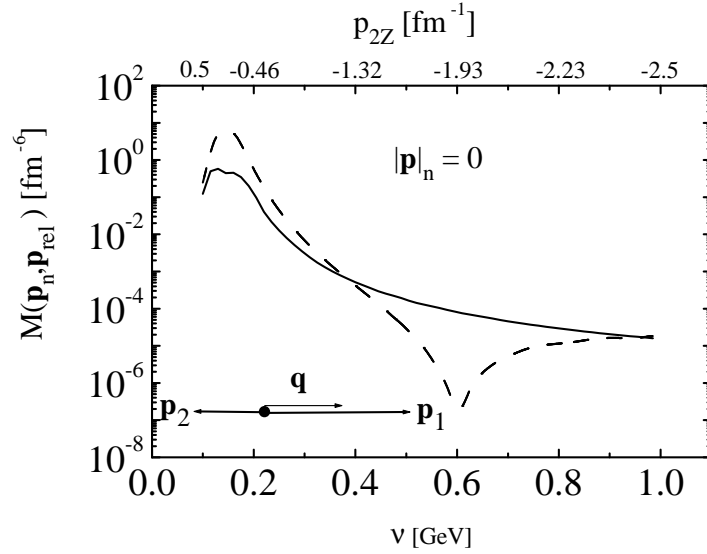


FIG. 5: The transition form factor $M(\mathbf{p}_n; \mathbf{p}_{rel}; \mathbf{q})$ (Eq.10) calculated in the Super-parallel kinematics ($p_{1z} = p_{2z} = 0, p_{1z} + p_{2z} = \mathbf{q} \cdot \hat{z}$, with $\mathbf{q} \parallel \hat{z}$). The dashed line corresponds to the Plane Wave Approximation (PWA) (plane waves for the three nucleons, Process (a) in Fig. 2), whereas the full line includes the pp rescattering (Process (a) + Process (b) in Fig. 2). The value of $\mathbf{q} \cdot \hat{z}$ corresponds to $E = 2 \text{ GeV}$ and $\theta = 15^\circ$ (cf. Eq. 1) and the range of its variation with v is $0.52 \text{ GeV} = c |\mathbf{q} \cdot \hat{z}| \leq 1.0 \text{ GeV} = c$. Three-body wave function from Ref. [19]; AV18 interaction [22].

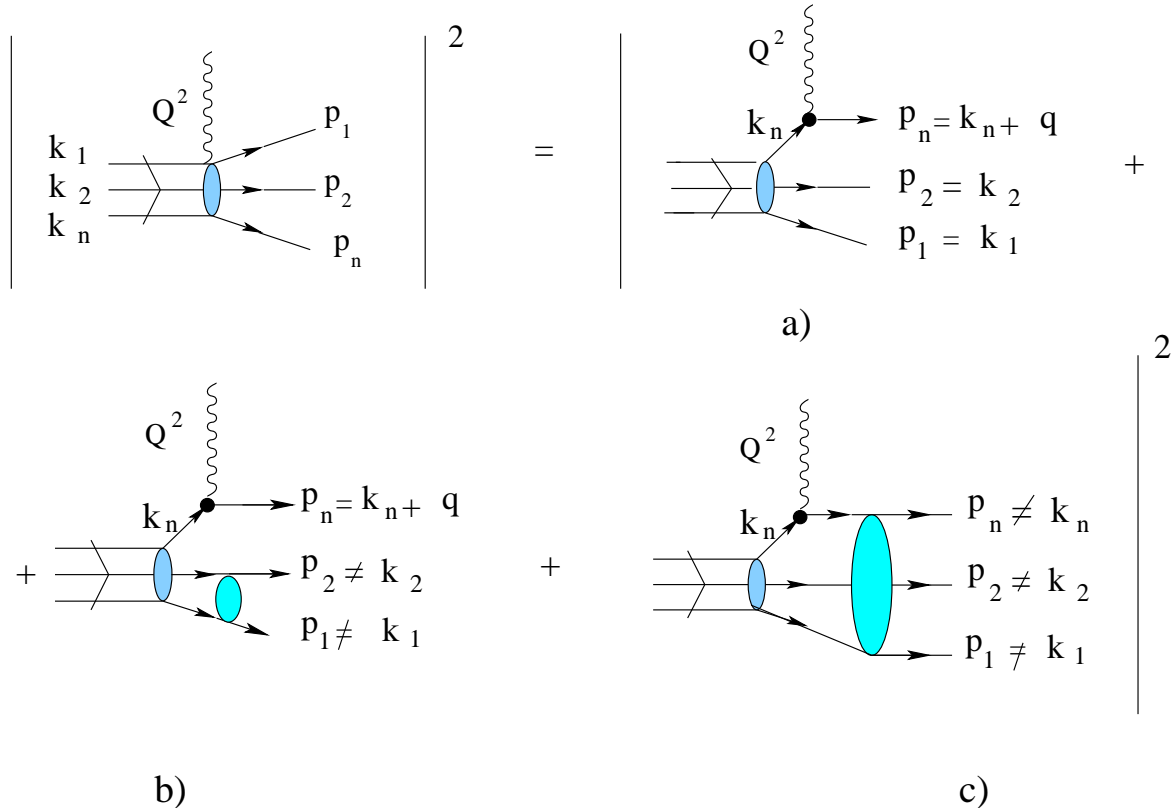


FIG. 6: Schematic representation of the various processes contributing to the reaction ${}^3\text{H} e(e;e'p_1p_2)n$ when Q^2 is absorbed by the neutron, and the two protons are emitted in the continuum: (a) denotes the Plane Wave Approximation (PWA), (b) the pp rescattering, (c) the three-body rescattering. The sum of contributions a) and b) is referred to by some authors as the Plane Wave Impulse Approximation (PWIA); in Ref. [6] PWIA is used, on the contrary, to denote our (symmetrized) PWA approximation. In the rest of this paper we shall be using the term PWA to denote process a), and the term pp rescattering to denote process b). Note moreover, that in Ref. [6] our pp rescattering contribution is called "tG₀".

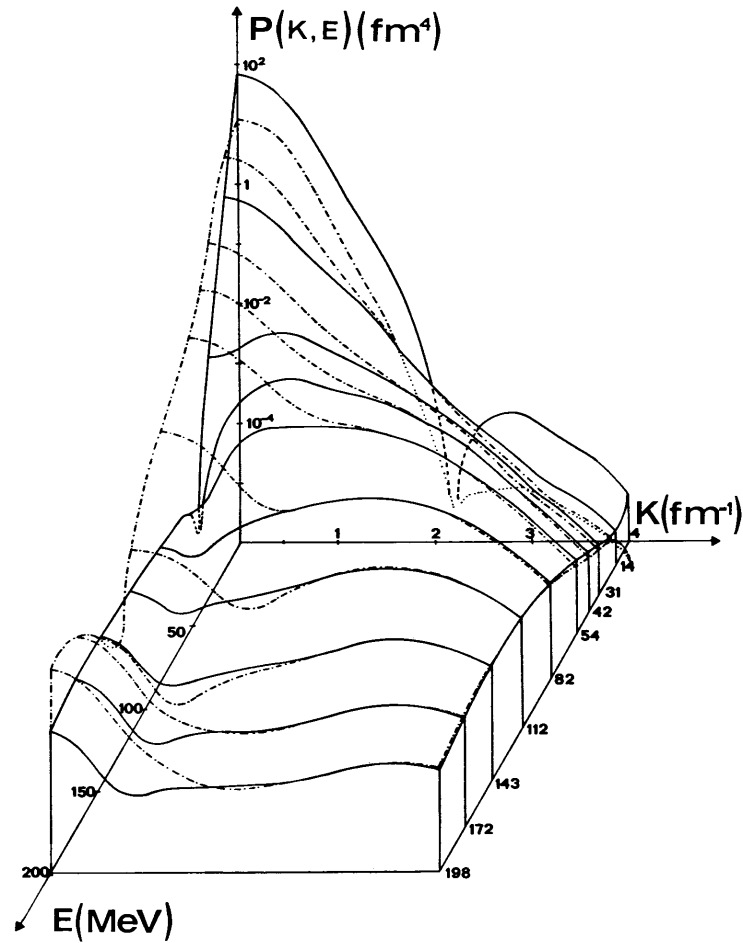


FIG. 7: The neutron Spectral Function in ${}^3\text{He}$ ($k = k_n$) corresponding to the three-body channel ${}^3\text{He} \rightarrow (pp) + n$. The dot-dashed line represents the PWA, whereas the full line includes the proton-proton rescattering. Three-nucleon wave function from [23]; Reid Soft Core interaction [25] (adapted from Ref. [23]).

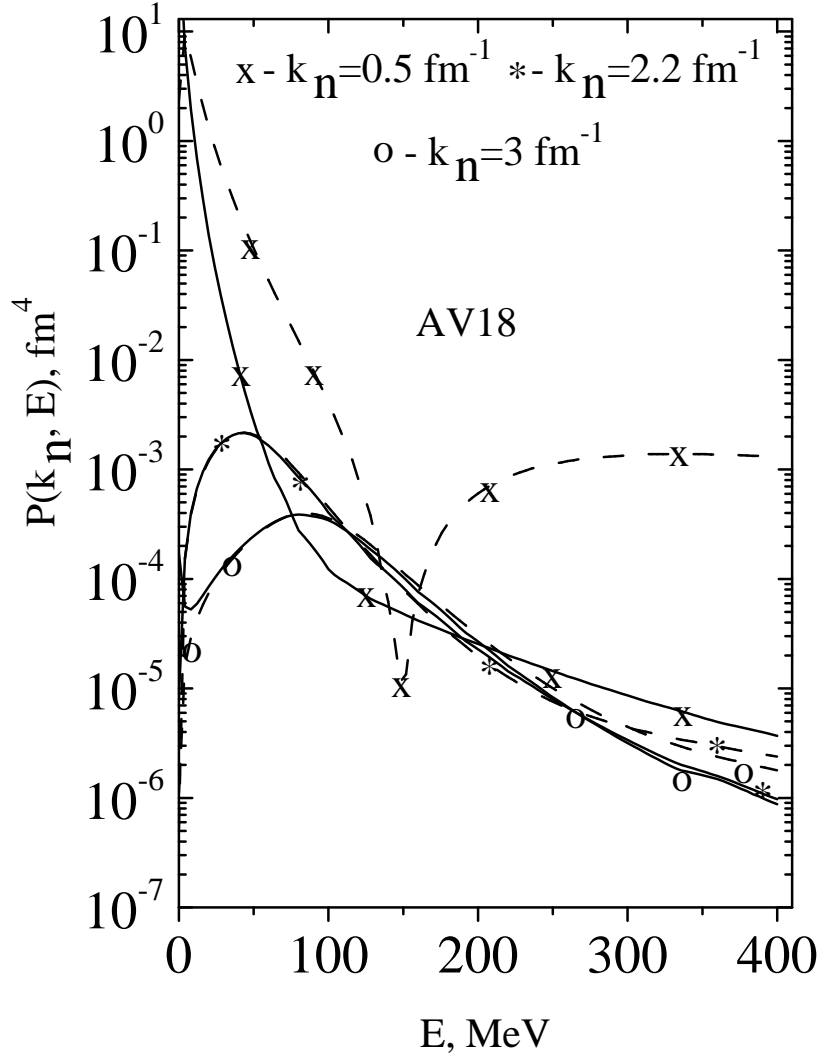


FIG . 8: The same as in Fig. 7 but with the three-body wave function from Ref. [19] and the AV18 interaction [22]. The E-dependence of the Spectral Function is shown for three values of the neutron momentum. The dashed line represents the PWA results, whereas the full line includes the pp rescattering.

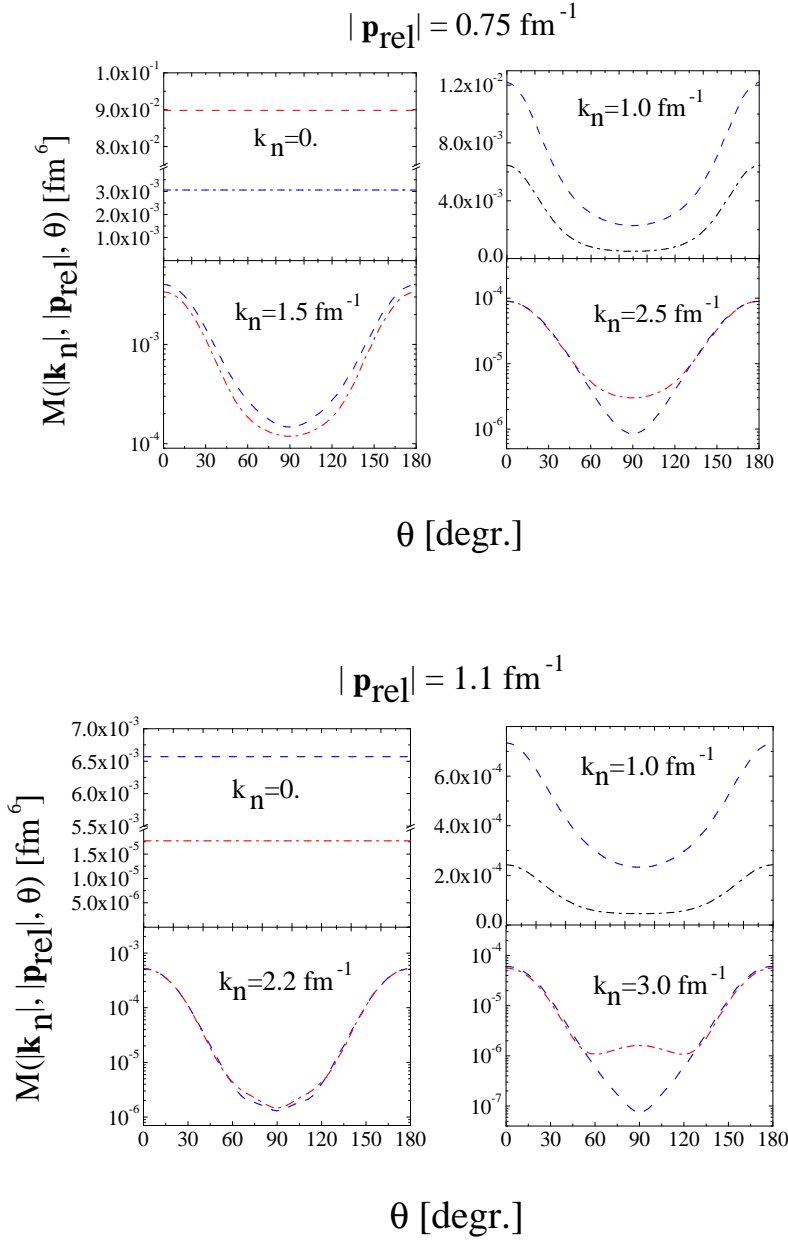


FIG. 9: Top panel. Dashed line: the transition form factor $M^{\text{pp}}(\mathbf{k}_n; \mathbf{p}_{\text{rel}}) = \frac{2}{M_N |\mathbf{p}_{\text{rel}}|} P_1(k_n; \mathbf{p}_{\text{rel}})$ (see Eq. 34) plotted vs the angle θ between \mathbf{k}_n and \mathbf{p}_{rel} for various values of $k_n = |\mathbf{k}_n|$ and $|\mathbf{p}_{\text{rel}}| = 0.75 \text{ fm}^{-1}$ (the corresponding "excitation energy" of the pp pair is $E = |\mathbf{p}_{\text{rel}}|^2 = M_N \cdot 23 \text{ MeV}$). Dot-dashed line: the same quantity in the PW A, i.e. disregarding the pp rescattering. Three-body wave function from Ref. [19]; AV18 interaction [22].

Bottom panel: the same as in Top panel for $|\mathbf{p}_{\text{rel}}| = 1.1 \text{ fm}^{-1}$ ($E = |\mathbf{p}_{\text{rel}}|^2 = M_N \cdot 50 \text{ MeV}$).

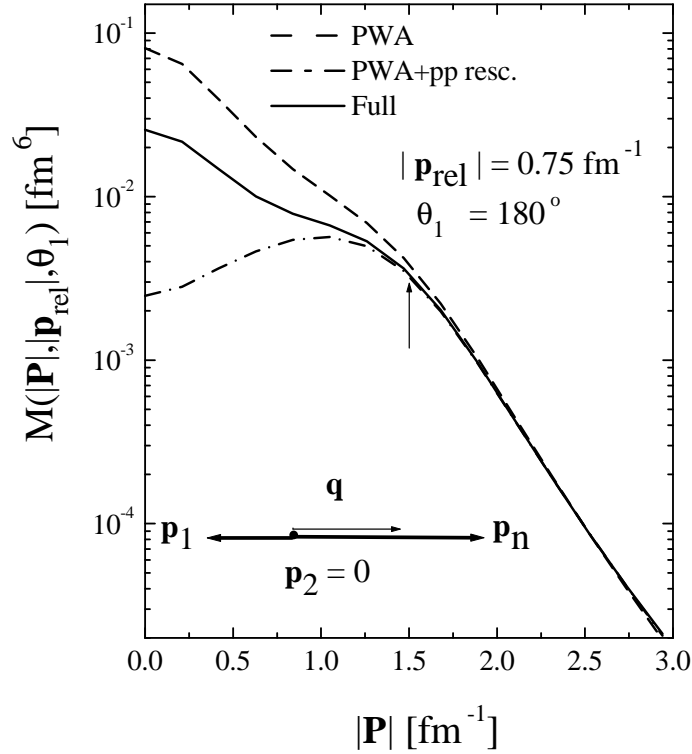


FIG. 10: The transition form factor $M(|\mathbf{P}|, |\mathbf{p}_{\text{rel}}|, \theta_1) = M(|\mathbf{p}_n|, |\mathbf{p}_{\text{rel}}|, \mathbf{q})$ (Eq.10), plotted vs the absolute value of the two-nucleon Center-of-Mass (or missing) momentum $|\mathbf{P}| = |\mathbf{p}_1 + \mathbf{p}_2| = |\mathbf{p}_m| = |\mathbf{p}_n|$ for fixed values of $|\mathbf{p}_{\text{rel}}| = 0.75 \text{ fm}^{-1}$ ($E = |\mathbf{p}_{\text{rel}}|^2 / M_N \approx 23 \text{ MeV}$) and the angle between \mathbf{q} and \mathbf{p}_{rel} , $\theta_1 = 180^\circ$ (note that in the PWA, as well as in the case when the pp rescattering is considered, $\theta_1 = 0^\circ$, since \mathbf{q} and \mathbf{k}_n can be chosen along \mathbf{q}). The dashed line represents the PWA (eq. 15), the dot-dashed line includes the pp rescattering (Eq.27), and the full line includes also the n(p) rescattering according to Eq. 42. Note that the results corresponding to the PWA ($\mathbf{p}_1 = \mathbf{k}_1, \mathbf{p}_2 = \mathbf{k}_2, \mathbf{p}_3 = \mathbf{k}_3 + \mathbf{q}$) and to the pp rescattering ($\mathbf{p}_3 = \mathbf{k}_3 + \mathbf{q}$), are the same as in Fig. 9 (with $\mathbf{k}_n = \mathbf{P}$). In these cases, the arrow and the momentum vector balance shown in the Figure denote the point where Eq. 38 is satisfied, i.e. $|\mathbf{k}_n| = 2|\mathbf{p}_{\text{rel}}| = 1.5 \text{ fm}^{-1}$, $k_1 = k_n, k_2 = 0$; it should be stressed that the dashed and dot-dashed lines, when $\theta_1 = 0^\circ$, would be exactly the same, with the arrow denoting in this case the configuration with $|\mathbf{k}_n| = 2|\mathbf{p}_{\text{rel}}|, k_2 = k_n, k_1 = 0$. The inclusion of the n(p) rescattering destroys in principle the $\theta_1 = 0^\circ - 180^\circ$ symmetry, but, as explained in the text, the asymmetry generated by our Glauber-type calculations is very mild. For $|\mathbf{P}| > 1.5 \text{ fm}^{-1}$, the ground-state configuration always corresponds to $|\mathbf{k}_n| = |\mathbf{k}_1|$ and $|\mathbf{p}_2|$ much smaller than $|\mathbf{k}_1|$ which means a configuration similar to the 2N C configuration, whereas for $0 < |\mathbf{P}| < 1.5 \text{ fm}^{-1}$, $|\mathbf{k}_1| \neq |\mathbf{k}_2|$ and $|\mathbf{k}_n| \neq 0$, which means a configuration far from the 2N C one. Three-nucleon wave function from [19]; AV18 interaction [22].

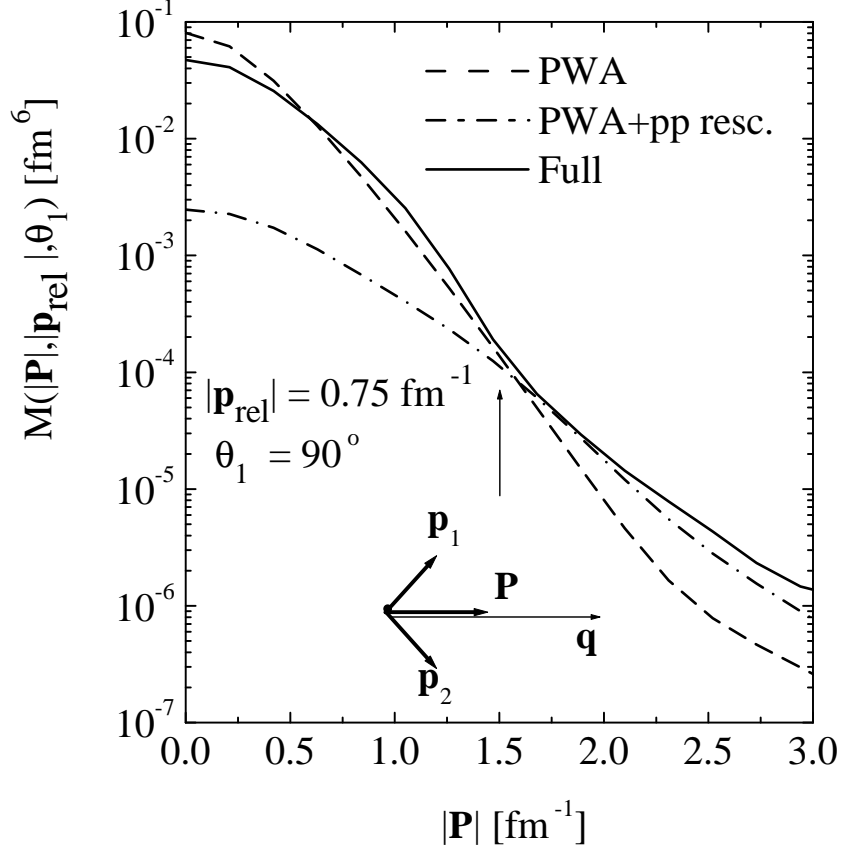


FIG. 11: The same as in Fig. 10 but for $\theta_1 = 90^\circ$ (cf. Fig. 9, as far as the dashed and dot-dashed lines are concerned). The arrow and the momentum vector balance correspond to the point where Eq. 38 is satisfied ($k_n \neq 2p_{\text{rel}} = 1.5 \text{ fm}^{-1}$), but since $\theta_1 \neq 0^\circ$ (180°), we do not stay now in the two nucleon correlation region, but rather in the three-nucleon correlation region, for $k_2 j' = k_1 j'$ $k_n \neq \frac{p}{2}$, 1.1 fm^{-1} (cf. Appendix 2). For $p > 1.5 \text{ fm}^{-1}$, e.g. at $p = 2.0 \text{ fm}^{-1}$, the ground-state configuration is such that $k_n j = 2 \text{ fm}^{-1}$, $k_{1(2)} j = 1.5 \text{ fm}^{-1}$, whereas for $p < 1.5 \text{ fm}^{-1}$, e.g. at $p = 0.5 \text{ fm}^{-1}$, one has $k_n j = 0.5 \text{ fm}^{-1}$ and $k_{1(2)} j = 0.8 \text{ fm}^{-1}$. Three-nucleon wave function from [19]; AV18 interaction [22].

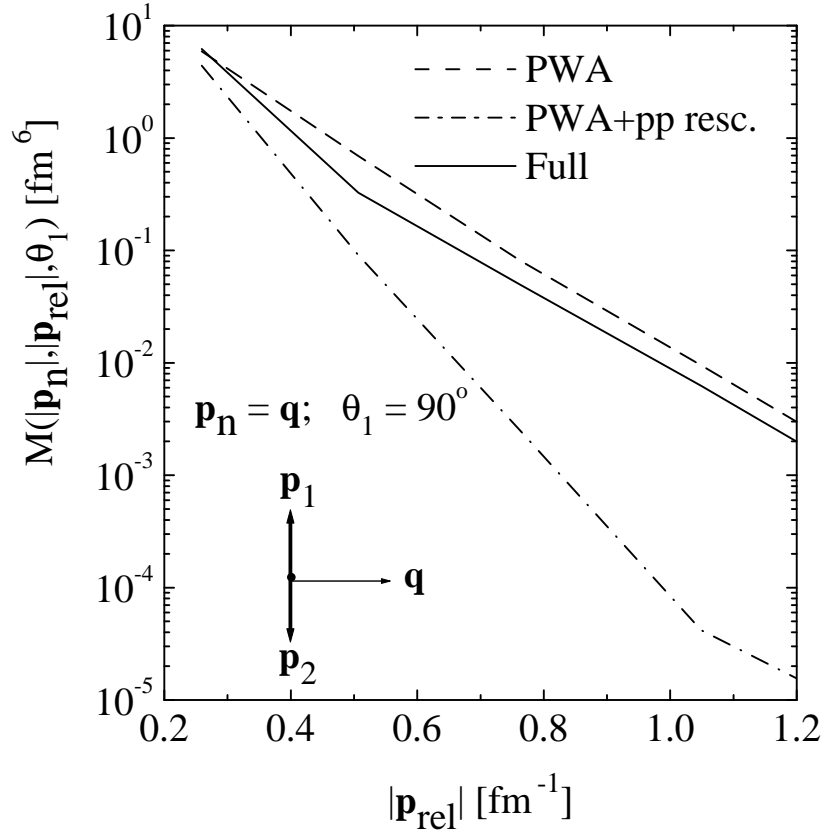


FIG. 12: The transition form factor $M(\mathbf{p}_n, |\mathbf{p}_{\text{rel}}|, \theta_1) = M(\mathbf{p}_n; \mathbf{p}_{\text{rel}}; \mathbf{q})$ (Eq. 10), plotted vs $|\mathbf{p}_{\text{rel}}|$ for $\mathbf{p}_n = \mathbf{q}$, $\theta_1 = 90^\circ$. The process corresponds to the absorption of \mathbf{q} by a neutron at rest followed by the emission of two protons with momenta $\mathbf{p}_1 = -\mathbf{p}_2$ (back-to-back protons). The dashed line represents the PWA (eq. 15), the dot-dashed line includes the pp rescattering (Eq. 27), and the full line includes also the n (pp) rescattering according to Eq. 42. The dashed and dot-dashed lines represent the ones in Fig. 9 at, $k_n = 0$, $\theta_1 = 90^\circ$ and all values of $0.2 \text{ fm}^{-1} < |\mathbf{p}_{\text{rel}}| < 1.2 \text{ fm}^{-1}$. Thus the dashed and dot-dashed lines coincide in both Figures. Note that the dashed line represents the three-body wave function in momentum space; it however differs from the dashed line in Fig. 3 where \mathbf{q} interacts with a proton of a correlated pair. Three-nucleon wave function from [19]; AV18 interaction.